Design of Index-Coupled DFB Lasers with Reduced Longitudinal Spatial Hole Burning

Geert Morthier and Roel Baets, *Member, IEEE*

Abstract—**Methods for reducing or eliminating longitudinal spatial hole burning in AR-coated, index-coupled DFB lasers are discussed. It is shown that elimination of spatial hole burning in DFB lasers can be achieved by the introduction of well-chosen variations of coupling strength and/or internal absorption in the longitudinal direction. Approximations for these structures are modeled numerically and fabrication methods for these approximate structures are suggested.**

I. Introduction

Optical communication systems require dynamic single-mode lasers with a narrow linewidth as transmitters and DFB lasers seem to be the favorite candidate among all laser types. Commonly used DFB lasers, when properly designed, can exhibit a stable single-mode behavior up to high-power levels. Unfortunately, for such lasers, which have a typical length of a few hundred micrometers, a linewidth below 5 MHz is not easily achieved. On the other hand, a lot of effort has been spent to achieve laser-diode linewidths below 1 MHz [1], which would allow to increase the data transmission rates.

Two possible ways for reducing the linewidth of DFB lasers are then the use of a larger coupling coefficient and the introduction of longer lasers. However, it has been found both experimentally [2] and theoretically [3] that lasers with a large coupling coefficient and/or large lengths often become multimode already at low or moderate power levels. This deterioration in side-mode suppression is due to longitudinal spatial hole burning (i.e., a nonuniform carrier density resulting from a nonuniform power density) which causes a longitudinal variation of the Bragg wavelength. This effect is generally more important in lasers with a large coupling coefficient and/or a large length. It can be noticed here that the presence of spatial hole burning in DFB lasers also influences the FM-response and may result in a less flat FM-response [4]. It also results in intermodulation distortion [5] (an unwanted effect in analog communication) and chirp. Furthermore, longitudinal spatial hole burning sometimes results in an increase of the linewidth, even if side modes remain well below threshold [6].

For this reason, special laser structures with reduced spatial hole burning have been and are still intensively investigated. Up to now, multiple-phase-shifted [7], [8] or chirped-grating lasers [9] have been considered as the best solution to this problem. It has also been shown recently that the introduction of gain coupling may lead to lasers with a high threshold gain difference and a reduced spatial hole burning [10], but the fabrication of such lasers is very difficult. Index-coupled lasers with uniform or nearly uniform optical power have been reported in [12] and [13], where two very specific structures are discussed.

In this paper, we present a more general account of how slow variations of the grating amplitude, the Bragg wavelength and/or of the net gain allow to eliminate spatial hole burning in index-coupled DFB lasers. In a first part, it is outlined how the coupled-wave equations can be transformed into equations from which structures with perfectly uniform power can readily be derived. It is shown that a theoretical laser structure with uniform power can always be obtained by choosing two arbitrary functions. A second part describes some of the more basic solutions with uniform power. We end by presenting more practical approximations of these structures, their numerical modeling and some methods to fabricate them. New structures with uniform power are added to the ones reported in [12] and [13], while furthermore our analysis allows interested readers to derive other structures with uniform power.

II. Theory

We restrict our analysis to index-coupled DFB lasers with perfectly AR-coated facets in order to avoid complications arising from the uncertainty in the facet phases. Our analysis can easily be extended to finite facet reflectivities if the phases are known, but the uncertainty in the phases makes it less interesting. Spatial hole burning effects are no longer present if the intracavity power is uniform in the longitudinal direction z. The intracavity field can be expressed in this case as

$$E(z) = R^+(z)e^{-j\beta_0(z)z} + R^-(z)e^{j\beta_0(z)z} \quad (1)$$

where $\beta_0(z) = \pi/\Lambda(z)$ represents the Bragg number and $\Lambda(z)$ is the grating period, assumed to be slowly varying

Manuscript received Feburary 21, 1991; revised May 2, 1991. This work was supported in part by the European RACE-projects R1010 (CMC) and R1069 (EPLOT). The work of G. Morthier was supported in part by the Belgian IWONL.

The authors are with the Laboratory of Electromagnetism and Acoustics, University of Gent-IMEC, St. Pietersnieuwstraat 41, B-9000 Gent, Belgium.

IEEE Log Number 9101624.

0733-8724/91/1000-1305$01.00

over one wavelength. The slowly varying amplitudes R^+ and R^- of the forward and backward propagating waves obey the coupled-wave equations [11]

$$\frac{dR^+}{dz} + [j\Delta\beta_r - \Delta\beta_i]R^+ = \kappa_{FB}(z)R^-(z) \tag{2a}$$

$$\frac{dR^-}{dz} - [j\Delta\beta_r - \Delta\beta_i]R^- = \kappa_{FB}^*(z)R^+(z). \tag{2b}$$

The Bragg deviation $\Delta\beta_r(z)$ and the net amplitude gain $\Delta\beta_i(z)$ are also assumed to be slowly varying functions of z. Such variations can take into account a possible variation of the grating period, a variation of the internal absorption or more generally any variation in the composition of the passive layers. The z dependence of the coupling coefficients incorporates, e.g., a possible variation of the grating amplitude.

It can easily be shown that the coupled-wave equations, which are usually derived for a longitudinally invariant waveguide geometry and a perfectly periodic grating, still hold for slowly varying functions $\Delta\beta_r(z)$, $\Delta\beta_i(z)$, and $\kappa_{FB}(z)$. One can derive a few relations that have to be fulfilled when a uniform power density is to be obtained. To this end, we introduce amplitudes and phases for the complex quantities κ_{FB}, R^+, and R^-

$$R^+ = r^+e^{j\varphi^+} \tag{3a}$$

$$R^- = r^-e^{j\varphi^-} \tag{3b}$$

$$\kappa_{FB} = \kappa e^{j\varphi_\kappa} \tag{3c}$$

where r^+, r^-, φ^+, φ^-, κ, and φ_κ are all real functions of z. $\varphi_\kappa(z)$ can be assumed to be piecewise constant, with changes in φ_κ occurring only at points where a phase shift in the grating is present. Furthermore, the perfect AR-coating of the facets allows to take $\varphi_\kappa = 0$ at $z = 0$.

The coupled-wave equations can be transformed into

$$\frac{dr^+}{dz} - \Delta\beta_i r^+ = |\kappa| r^- \cos(\varphi_\kappa + \varphi^- - \varphi^+) \tag{4a}$$

$$\frac{dr^-}{dz} + \Delta\beta_i r^- = |\kappa| r^+ \cos(\varphi_\kappa + \varphi^- - \varphi^+) \tag{4b}$$

$$\frac{d\varphi^+}{dz} + \Delta\beta_r = |\kappa| \frac{r^-}{r^+} \sin(\varphi_\kappa + \varphi^- - \varphi^+) \tag{4c}$$

$$\frac{d\varphi^-}{dz} - \Delta\beta_r = -|\kappa| \frac{r^+}{r^-} \sin(\varphi_\kappa + \varphi^- - \varphi^+). \tag{4d}$$

Complete elimination of spatial hole burning is possible only if a variable coupling constant and/or if a variable gain/loss is allowed. This can easily be shown theoretically with the help of the coupled-wave equations. Multiplication of (4a) with r^+, of (4b) with r^- and addition of both resulting equations gives an equation for the z variation of the optical power $(r^+) + (r^-)^2$, from which it follows that a uniform power requires the following relation:

$$2|\kappa| \cos(\varphi_\kappa + \varphi^- - \varphi^+) = \Delta\beta_i \frac{(r^-)^2 - (r^+)^2}{r^+r^-}. \tag{5}$$

The denominator on the r.h.s. of (5) approaches infinity if one or both facets are perfectly AR-coated. The requirement can then only be fulfilled if $|\kappa(z)|$ approaches infinity as well or if $\Delta\beta_i(z)$ vanishes at this facet. The case with $\Delta\beta_i(z)$ being identically zero is not really of interest and nor is the case with $|\kappa(z)|$ being identically infinite. Both cases actually correspond with lasers with zero efficiency (i.e., no output power can be extracted).

Structures with uniform optical power can be derived after transformation of the coupled-wave equations in the following way. We first note that the perfect AR-coating of the facets and the requirement of a uniform power can be expressed by the following relations:

$$r^+(0) = r^-(L) = 0. \tag{6a}$$

$$[r^+(z)]^2 + [r^-(z)]^2 = 1. \tag{6b}$$

The power is normalized here. A first useful equation can now be derived by multiplication of (4a) with r^+, multiplication of (4b) with r^-, and subtraction of both equations:

$$\frac{d(r^+)^2}{dz} - 2\Delta\beta_i(r^+)^2 = \frac{d(r^-)^2}{dz} + 2\Delta\beta_i(r^-)^2. \tag{7}$$

Taking into account the relation (6b) readily gives

$$\frac{d(r^+)^2}{dz} = \Delta\beta_i \tag{8}$$

and integration of this last equation gives

$$\int_0^L \Delta\beta_i(z)\, dz = 1. \tag{9}$$

The power of forward and backward propagating waves is then found to be

$$(r^+)^2 = \int_0^z \Delta\beta_i(z')\, dz'; \qquad (r^-)^2 = \int_z^L \Delta\beta_i(z')\, dz'. \tag{10}$$

Substitution of these functions into (5) shows that the right-hand side is completely determined. Equation (5) allows to determine the required coupling coefficient, provided the phase difference is known. An equation for this phase difference can be derived from (4c) and (4d)

$$\frac{d(\varphi^- - \varphi^+)}{dz} - 2\Delta\beta_r = -\Delta\beta_i \frac{[1 - 2(r^+)^2]}{2(r^+)^2(r^-)^2} tg(\varphi_\kappa + \varphi^- - \varphi^+). \tag{11}$$

It must be noticed that, due to the AR-coating of the facets, only this phase difference has a physical meaning. The phase $\varphi_\kappa(z)$ can be considered as a stepwise constant function. Continuous changes in this phase can be included in $\Delta\beta_r(z)$ since they can also be regarded as changes in the grating period. In fact, phase jumps as in phase-shifted lasers could also be included in $\Delta\beta_r(z)$ as Dirac functions.

Several structures with a uniform power density can now be derived from (8)–(11), just by choosing appropriate functions for $\Delta\beta_i(z)$, $\kappa(z)$, and $\Delta\beta_r(z)$. Two of these functions, e.g., $\Delta\beta_i(z)$ and $\Delta\beta_r(z)$, can be chosen freely. It can be seen however that (11) is easier to solve if $\Delta\beta_r(z)$ is replaced by another function

$$\Delta\beta_r(z) = \frac{f(z)}{\cos(\varphi_\kappa + \varphi^- - \varphi^+)};$$

$$y = \sin(\varphi_\kappa + \varphi^- - \varphi^+) \qquad (12a)$$

yielding for (4.3.8)

$$\frac{dy}{dz} + \Delta\beta_i(z)\frac{[1 - 2(r^+)^2]}{2(r^+)^2(r^-)^2}\, y = 2f(z). \qquad (12b)$$

The last equation is a first-order linear differential equation, which, for a given f, is easily solved. Hence, by choosing functions for $f(z)$ and $\Delta\beta_i(z)$, one can determine the fields and the phases. The required variations of κ and $\Delta\beta_r$ then follow from (5) and (12a).

III. Exact Solutions

A. Solutions with Constant $\Delta\beta_i$

For this case, one readily finds from (9) and (10)

$$\Delta\beta_i(z) = 1/L \quad \text{and}$$

$$r^+(z) = \sqrt{z/L}; \quad r^-(z) = \sqrt{1 - z/L}. \qquad (13)$$

The power of forward and backward propagating beams varies linearly in the longitudinal direction. A simple solution of (11) is then

$tg(\varphi_\kappa + \varphi^- - \varphi^+) = c$, with c an arbitrary real constant

$$\Delta\beta_r(z) = \frac{\left(1 - 2\frac{z}{L}\right)}{4L\frac{z}{L}\left(1 - \frac{z}{L}\right)}\, c. \qquad (14)$$

The $\kappa(z)$-function can be derived from (5). It follows that a phase shift of π is needed at $z = L/2$ in order to keep $|\kappa(z)|$ positive and one finds for $\kappa(z)$

$$\kappa(z) = \frac{1}{2L}\frac{\left(1 - 2\frac{z}{L}\right)}{\sqrt{\frac{z}{L}\left(1 - \frac{z}{L}\right)}}\sqrt{1 + c^2}. \qquad (15)$$

The variation of $\Delta\beta_r$ can practically result from a variation in, e.g., the composition of the cladding layers (although usually this also implies a small variation of α_{int}) or the grating period. An interesting special case rises when c is chosen zero. Both $\Delta\beta_i$ and $\Delta\beta_r$ are then constant and the solution corresponds to a uniform waveguide geometry, where the amplitude of the grating varies in the longitudinal direction [13]. Lasing occurs at the Bragg wavelength in this case.

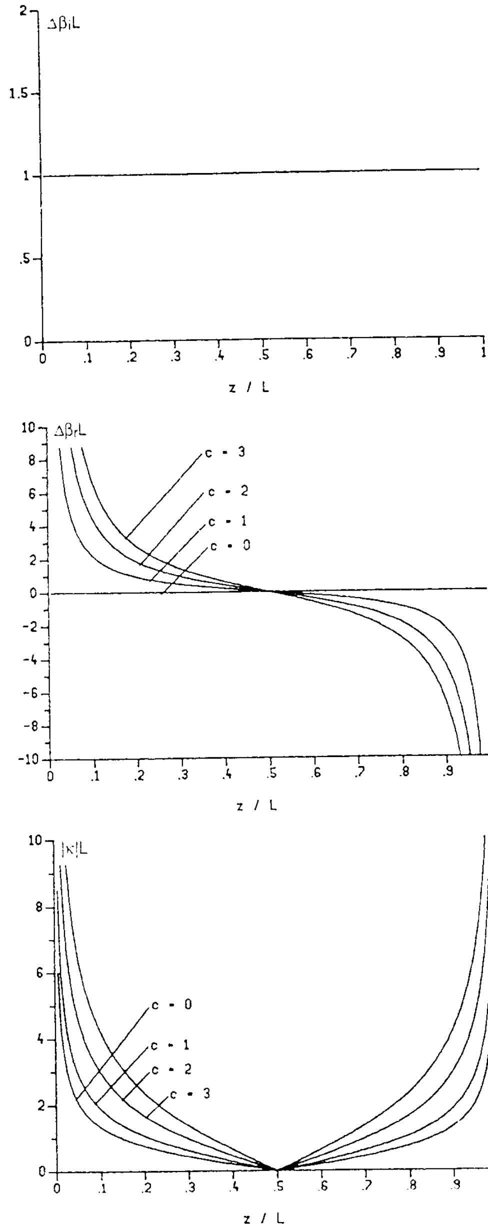

Fig. 1. The functions $\Delta\beta_i$, $\Delta\beta_r$, and $|\kappa|$ for the structure described by (13)–(15); for $c = 0$, $c = 1$, $c = 2$, and $c = 3$.

The functions $\Delta\beta_r(z)$, $\Delta\beta_i(z)$, and $|\kappa(z)|$ are displayed in Fig. 1 for different values of the parameter c. Both $\Delta\beta_r(z)$ and $|\kappa(z)|$ increase with increasing values of c, which is not surprising since an increase of the Bragg deviation (or of the value of c) results in a weakening of the distributed reflections and must be compensated by an increase of the required coupling coefficient. The low value of $|\kappa(z)|$ in the central region of the laser prevents a power concentration in this region. There is little reflection in this region and the longitudinal variation of the power of forward and backward propagating waves seems to have its origin in stimulated emission there. This stimulated emission would cause a power concentration near the facets (as in Fabry–Perot lasers), which, however, is prevented by the growing reflection as $|\kappa(z)|$ increases.

B. Solutions With Variable $\Delta\beta_i$

To remove the singularity in the $\kappa(z)$ function, one can try a solution of the form

$$\Delta\beta_i(z) \sim r^+(z) r^-(z). \quad (16)$$

The solutions are

$$r^+(z) = \sin\left(\frac{(2n+1)\pi z}{2L}\right);$$

$$r^-(z) = \cos\left(\frac{(2n+1)\pi z}{2L}\right) \quad (17a)$$

$$\Delta\beta_i(z) = \frac{(2n+1)\pi}{2L}\sin\left(\frac{(2n+1)\pi z}{L}\right) \quad (17b)$$

with n an integer. From (11), one can see that again a solution with $\Delta\beta_r(z) = 0$ exists. Again, a phase shift of π at $z = L/2$ is required to keep $|\kappa(z)|$ positive and one finds

$$\kappa(z) = \frac{(2n+1)\pi}{2L}\cos\left(\frac{(2n+1)\pi z}{L}\right). \quad (18)$$

This structure with $n = 0$ has been reported also in literature [12]. It must be noticed once more that the variation of $\Delta\beta_i$ (which can be implemented as a variation of the absorption or as a variation of the gain) will often be accompanied by a variation of $\Delta\beta_r$. This is the case when a variable composition of the passive layers (i.e., a variable loss in the passive layers) or a nonuniform injection is applied. The variations of $\Delta\beta_r$ should then be restricted or compensated for (e.g., by an appropriate variation of the grating period).

The functions $\Delta\beta_r(z)$, $\Delta\beta_i(z)$, and $|\kappa(z)|$ are depicted in Fig. 2 for $n = 0$ and $n = 1$. For the case $n = 0$, we can again argue that the low $|\kappa|$-value near $z = L/2$ prevents a power concentration in the center of the laser. The concentration of power near the facets on the other hand is now anticipated by both the increase of $|\kappa(z)|$ and the decrease of $\Delta\beta_i(z)$ (i.e., the net stimulated emission rate is reduced and the reflections become stronger).

Other structures, for which the variation of $\Delta\beta_i$ and of r^+ and r^- is nonetheless again given by (17), can be derived after substitution of f in (12b) by

$$f(z) = c\left[\sin\left(\frac{(2n+1)\pi z}{L}\right)\right]^k \cos\left(\frac{(2n+1)\pi z}{L}\right) \quad (19)$$

with c being an arbitrary real constant and k an arbitrary integer. The solution of (12b) for this choice of $f(z)$ becomes

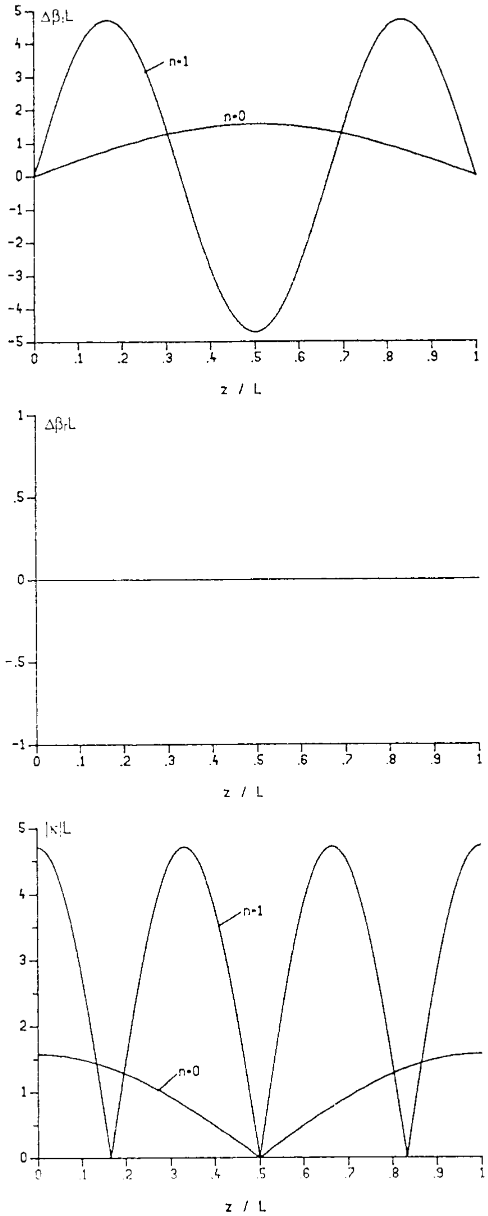

Fig. 2. The functions $\Delta\beta_i$, $\Delta\beta_r$, and $|\kappa|$ for the structure described by (17b) and (18); for $n = 0$ and $n = 1$.

$$y(z) = \frac{2c\left[\sin\left(\frac{(2n+1)\pi z}{L}\right)\right]^{k+1}}{(2n+1)(k+2)\pi/L} \quad \text{with}$$

$$a = \frac{2cL}{(2n+1)(k+2)\pi} \leq 1. \quad (20)$$

The last requirement thereby follows from (12a) (the cosine must have an amplitude below 1). From y and f, the Bragg deviation can be determined via (12a). It is, however, not possible to determine the sign of cos $(\varphi_\kappa + \varphi^- - \varphi^+)$ from (20). Both the + and − sign, as well as changes of the sign along the longitudinal axis are principally allowed. It must nevertheless be assured that the value of $|\kappa(z)|$ remains positive (e.g., by including phase shifts φ_κ). For the case $a = 1$ and $n = 0$, one finds the $\kappa(z)$ and $\Delta\beta_r(z)$

$$\Delta\beta_r(z) = \pm \frac{(k+2)\dfrac{\pi}{L}\left[\sin\left(\dfrac{\pi z}{L}\right)\right]^k}{\sqrt{1 + \left[\sin\left(\dfrac{\pi z}{L}\right)\right]^2 + \cdots + \left[\sin\left(\dfrac{\pi z}{L}\right)\right]^{2k}}} \tag{21a}$$

$$|\kappa(z)| = \frac{\pi}{2L} \frac{1}{\sqrt{1 + \left[\sin\left(\dfrac{\pi z}{L}\right)\right]^2 + \cdots + \left[\sin\left(\dfrac{\pi z}{L}\right)\right]^{2k}}}. \tag{21b}$$

The cases with $k = 0$ and $k = 1$ are of most interest. For $k = 0$, one finds a uniform $\kappa(= \pi/2L)$ and lasing at the average Bragg wavelength if $\Delta\beta_r(z)$ is chosen as

$$\Delta\beta_r(z) = \frac{\pi}{L} \qquad \text{for } 0 \leq z \leq L/2$$

and

$$\Delta\beta_r(z) = -\frac{\pi}{L} \qquad \text{for } L/2 \leq z \leq L \tag{22}$$

and if a $\lambda/4$ phase shift is introduced at $z = L/2$. For $k = 1$, one finds that $\Delta\beta_r$ and $\Delta\beta_i$ vary in a similar way along the longitudinal axis, while the variation of κ is rather small.

$$\Delta\beta_r(z) = \frac{\pm 3\Delta\beta_i(z)}{\sqrt{1 + \left[\sin\left(\dfrac{\pi z}{L}\right)\right]^2}} \tag{23a}$$

$$|\kappa(z)| = \frac{\pi}{2L} \frac{1}{\sqrt{1 + \left[\sin\left(\dfrac{\pi z}{L}\right)\right]^2}}. \tag{23b}$$

It must be emphasized that the previous solutions are not necessarily the modes with the lowest threshold gain (current), nor has it been proven that the special structures are single mode. Only when the uniform power solution is the main and only mode will there be an absence of spatial hole burning effects in the laser behavior. This can be expected for the solutions lasing at the average Bragg wavelength. The solutions with variable $\Delta\beta_i$, especially the cases where $n \neq 0$, seem to be higher order modes which might not be the main mode.

The variations of $|\kappa|$, $\Delta\beta_i$, and $\Delta\beta_r$ are shown in Fig. 3, respectively, Fig. 4 for the solutions (22), respectively (23). For these solutions, the values of $|\kappa(z)|$ are less small near $z = L/2$, but the distributed reflections there are suppressed by the large Bragg deviation. The Bragg deviation decreases near the facets for the solution (23). This results in increased reflections, which, together with the reduction of the net stimulated emission, once more prevent the power from concentrating near the facets.

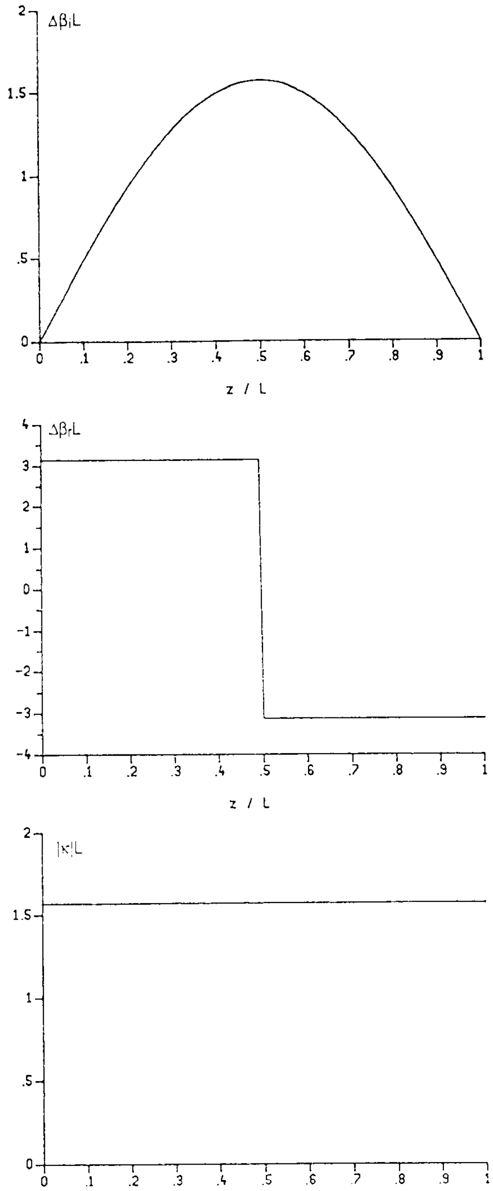

Fig. 3. The functions $\Delta\beta_i$, $\Delta\beta_r$, and $|\kappa|$ for the structure described by (17b) with $n = 0$ and (22).

Many other solutions could still be found by choosing appropriate functions for $f(z)$ and $\Delta\beta_i(z)$. For the case of a uniform $\Delta\beta_i$, e.g., one can also find solutions of (12b) if $f(z)$ is chosen as

$$f(z) \sim \left(1 - 2\frac{z}{L}\right)\left[\frac{z}{L}\left(1 - \frac{z}{L}\right)\right]^\alpha,$$

$$\alpha \text{ a positive real number.} \tag{24}$$

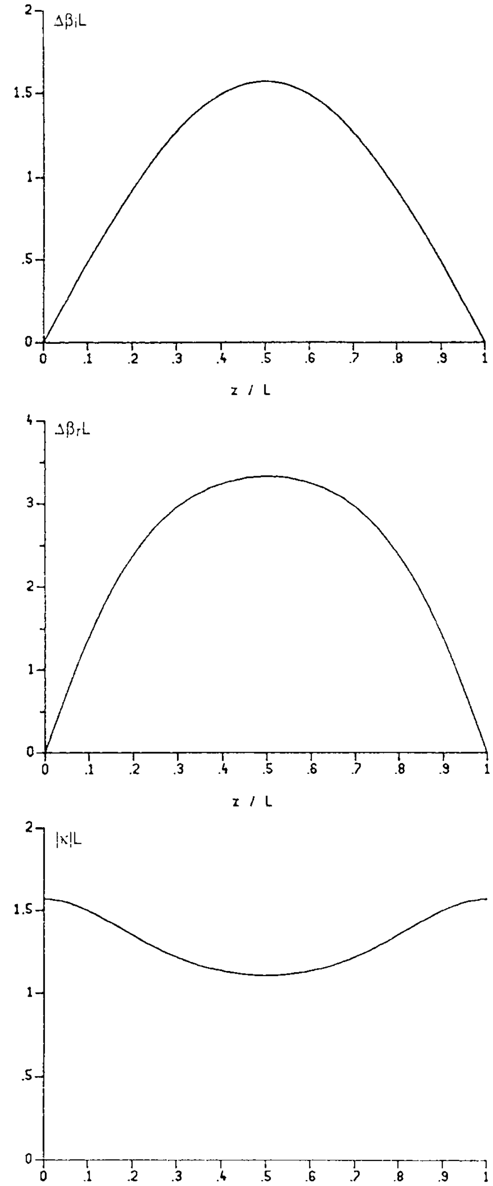

Fig. 4. The function $\Delta\beta_i$, $\Delta\beta_r$, and $|\kappa|$ for the structure described by (17b) with $n = 0$ and (23).

For $\Delta\beta_i(z)$, one can take other functions which vanish at $z = 0$ and $z = L$ (so that the singularities in $\kappa(z)$ disappear), e.g.,

$$\Delta\beta_i(z) = \left(\frac{z}{L}\right)^{\alpha}\left[1 - \left(\frac{z}{L}\right)^{\alpha}\right]. \tag{25}$$

A further exploration of possible structures with uniform power is left to the creativity of the interested reader. It is indeed not excluded that more interesting solutions exist. We also note that other solutions may be more difficult to obtain from a mathematical point of view, but may be easier to fabricate. However, we also believe that most other solutions will be based on a reduction of the distributed feedback (e.g., a large Bragg deviation or a small coupling coefficient) in the central part of the laser and a reduction of the net stimulated emission or an enhancement of the distributed feedback near the laser facets. For example, for the choice (25), one can derive solutions that are similar (but with rational instead of trigonometric functions) to the solutions corresponding with (17b).

IV. Approximations and Simulations

The previous exact solutions are probably very hard to realize in practice. We therefore carried out numerical simulations of some approximate structures that can be derived from the exact solutions. The numerical simulations are carried out with the help of the laser-diode simulator CLADISS, a laser model that can handle the analysis of most types of multisection lasers.

A. Solutions with Constant $\Delta\beta_i$

For $c = 0$, one finds a laser with a grating, the amplitude of which varies in the longitudinal direction [13]. The $\kappa(z)$ variation can then, e.g., be approximated by a linear, a cosine or a stepwise constant function. As a matter of fact, the function can be approximated to any degree if gratings are written by *e*-beam lithography. One can either vary the actual grating amplitude or the duty cycle of the grating [13]. A stepwise constant approximation has been analyzed in [13]. The approximation described there already results in an extremely uniform optical power, with variations that are restricted to 5%. For the threshold gain difference ΔgL, one finds the value 0.17 and therefore, a stable single-mode behavior should be observed for this structure.

A second approximation can be formed by the double exposure of a photoresist to form two holographic interference patterns of slightly different periods Λ_1 and Λ_2 ([14], [15]). This results in a cosine variation of κ. However, the variation of the coupling coefficient will in general be accompanied by a variation of the effective refractive index (and of the Bragg deviation) if the last method is used [13]. The relation between the variation of the coupling coefficient and that of the refractive index depends on the lithography and etching process. We have shown before [13] that the variation of the optical power is still restricted to about 10% and that a good mode rejection can still be expected even if a realistic longitudinal variation of the refractive index is present.

A last approximation, worthwhile mentioning, is a stepwise constant approximation with κ being constant in the outer sections and zero (i.e., no grating) in the central section. One must thereby assure that the π-phase shift between both gratings near the facets is still present. One possibility is to fabricate a $\lambda/4$-shifted grating and to remove the central part of it afterwards.

B. Solutions With Variable $\Delta\beta_i$

The structures for which $\Delta\beta_i$ varies in the longitudinal direction, but where $\Delta\beta_r$ must remain constant seem to be of purely theoretical interest. Indeed, it is not possible to produce variations in the gain or the absorption without having an additional variation in the effective refractive index, while, on the other hand, the compensation of such $\Delta\beta_r$ variations with the help of grating period variations complicates the fabrication to a large degree.

For the structure described by (17) and (18) with $n = 0$ however, one could speculate that the variation of κ (if produced by means of the double exposure technique) and the variation of $\Delta\beta_i$ will each be accompanied by $\Delta\beta_r$ variations that cancel each other. The variation of the power for a stepwise constant approximation of (17) and (18) (with eight sections of 37.5 μm) is shown in Fig. 5 for a 300-μm-long laser. We further remark that this structure (i.e., the stepwise constant approximation) exhibits a high ΔgL-value of ± 0.46.

The solution, described by (22), consists of a variable $\Delta\beta_i$, two different grating periods and a constant κ. The variation of the optical power for a stepwise constant approximation (again with eight sections of 37.5 μm) for the absorption is shown in Fig. 6 for a 300-μm-long laser. The grating periods have been chosen as $\Lambda_1 = 241.3$ nm and $\Lambda_2 = 240.9$ nm. The value of ΔgL now is given by 0.74. One can remark that the power variations in both Figs. 5 and 6 are restricted to 5%.

Two simple structures can further be obtained from approximations of (22), respectively (23). For the case (22), e.g., one can approximate $\Delta\beta_i(z)$ by a constant and divide the laser into two halfs with different grating periods, and separated by a $\lambda/4$-shift. We have modeled such a 300-μm-long laser with grating periods $\Lambda_1 = 241.3$ nm and $\Lambda_2 = 240.9$ nm. For the uniform $\Delta\beta_i$, one finds an optimum κL-value of 1.75 (instead of $\pi/2$). Fig. 7 depicts the longitudinal variation of the power. A value of 0.66 was found for ΔgL.

The solution (23) can be fabricated by introducing a stepwise (or other) variation of $\Delta\beta_i$, which is accompanied by a $\Delta\beta_r(z) \sim \pm 3\Delta\beta_i(z)$ and by approximating $\kappa(z)$ by a constant. In practice, variations in the absorption (or in the composition of the cladding layers) are indeed accompanied by variations of the refractive index of this order of magnitude. If the variation of $\Delta\beta_i$ is implemented as, e.g., a nonuniform injection, one has $\Delta\beta_r(z) = -\alpha\Delta\beta_i(z)$, with α being the linewidth enhancement factor. By using proper materials and/or by applying detuning, a value of ± 3 can be achieved for α. Another method of achieving the required variations in both $\Delta\beta_i$ and $\Delta\beta_r$ is by varying the width and/or the thickness of the active layer or the stripe width. Fig. 8 shows simulation results for a 300-μm-long structure, that is a stepwise constant approximation (with five steps) of the required $\Delta\beta_i$-function (implemented as an absorption variation) and for which $\Delta\beta_r = -3\Delta\beta_i$. The uniform value of κL has been optimized and is thus different from $\pi/2$. The optimum value was found to be $\kappa L = 1.455$. The power variations are again restricted to 5% and a ΔgL value of 0.22 is achieved.

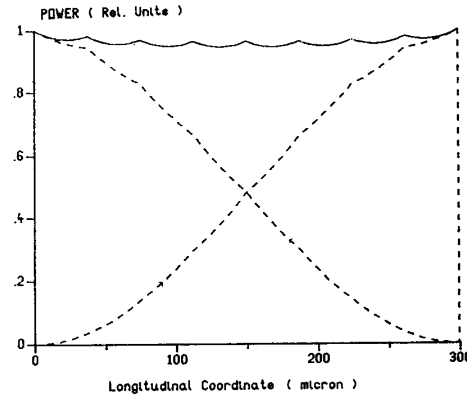

Fig. 5. Longitudinal variation of the optical power for a stepwise constant approximation (with eight sections of 37.5 μm) of the solution described by (18) ($n = 1$).

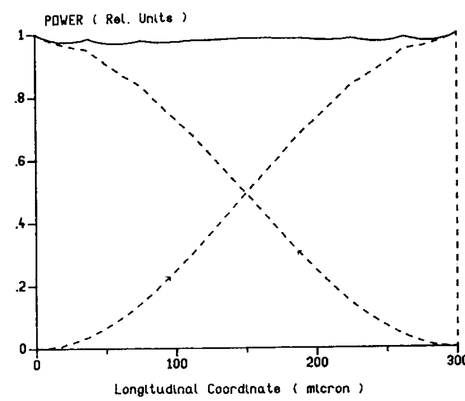

Fig. 6. Longitudinal variation of the optical power for a stepwise constant approximation (with eight sections of 37.5 μm) of the solution described by (22) ($n = 1$).

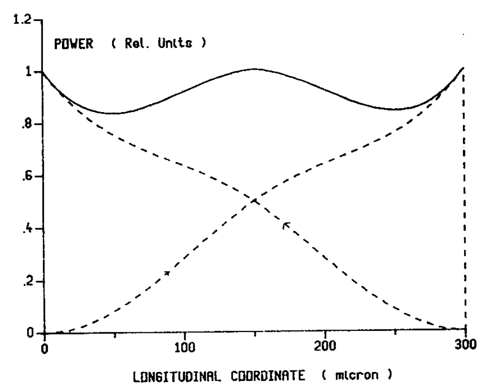

Fig. 7. Longitudinal variation of the optical power for a laser with two different grating periods Λ_1 and Λ_2 (separated by a $\lambda/4$-phase shift), with $\Lambda_1 = 241.3$ nm and $\Lambda_2 = 240.9$ nm.

Similar solutions can be found for $\alpha = 4, 5, \cdots$; e.g.,

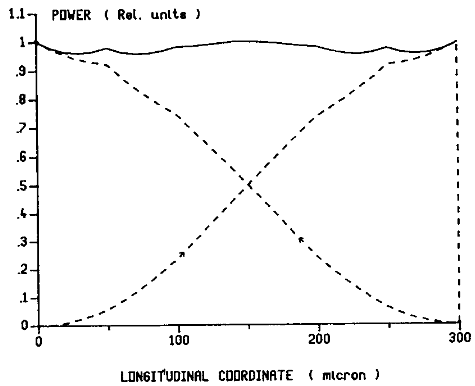

Fig. 8. Longitudinal variation of the optical power for a stepwise constant approximation (with five sections of 60 μm) of the solution (23), in which the denominators have been neglected (and hence for which $\kappa L = 1.455$ is a constant).

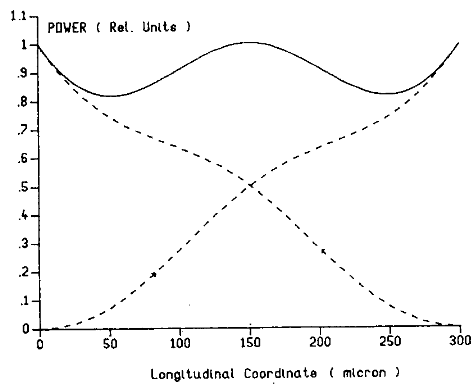

Fig. 9. Longitudinal variation of the optical power for a stepwise constant approximation (with five sections of 60 μm) of the solution (23), for which the variations of κ and $\Delta\beta_i$ have been neglected ($\kappa L = 1.6$).

starting from the functions (21) with $k = 2, 3, \cdots$. However, the z dependence of the denominator in (21) becomes more important in this case and if a constant $|\kappa|$ were applied, the power would be less uniform. Furthermore, by neglecting also the longitudinal variation of $\Delta\beta_i$, one arrives at chirped grating lasers. The variations of the optical power are now larger then for the previous structures, but they are still smaller than for ordinary or phase-shifted DFB lasers. Fig. 9 shows the longitudinal variation of the power for a 300-μm-long laser where $\Delta\beta_r(z)$ is a stepwise constant approximation (with five steps) of the function (23a), while κ and $\Delta\beta_i$ are constant along the laser axis. The optimum value of κL is found to be 1.6, yielding power variations that are restricted to 10% and a ΔgL-value of 0.25.

V. Conclusion

A number of new DFB-laser structures with both reduced longitudinal spatial hole burning and a large threshold gain difference have been discussed. It has been shown that spatial hole burning can be completely eliminated by the introduction of a longitudinally variable coupling coefficient and/or net gain. Several realistic devices, which can be relatively easily fabricated and in which the spatial hole burning is relatively small, have been modeled numerically.

The reduction of spatial hole burning often requires that the distributed feedback is weak and that the stimulated emission is large in the central laser region and that strong feedback and small stimulated emission exist near the facets. As the distributed feedback increases with increasing coupling coefficient and with decreasing Bragg deviation, the above described variations of κ, $\Delta\beta_i$, and $\Delta\beta_r$ are easily understood. With these arguments, one can also understand why nonuniform injection or grating period variations are capable of eliminating spatial hole burning effects to some extent.

Acknowledgment

The authors wish to acknowledge K. David and J. Buus for valuable discussions and suggestions.

References

[1] S. Ogita, Y. Kotaki, M. Matsuda, Y. Kuwahara, and H. Ishikawa, "Long-cavity, multiple-phase-shift distributed feedback laser for linewidth narrowing," *Electron. Lett.*, vol. 25, pp. 629–630, 1989.

[2] H. Soda, Y. Kotaki, H. Sudo, H. Ishikawa, and S. Yamakoshi, "Stability on single longitudinal mode operation in GaInAsP/InP phase-adjusted DFB lasers," *IEEE J. Quantum Electron.*, vol. QE-23, pp. 804–814, 1987.

[3] P. Vankwikelberge, G. Morthier, and R. Baets, "CLADISS, a longitudinal, multi-mode model for the analysis of the static, dynamic and stochastic behavior of diode lasers with distributed feedback," *IEEE J. Quantum Electron.*, Oct. 1990.

[4] P. Vankwikelberge *et al.*, "Analysis of the carrier induced FM response of DFB lasers: Theoretical and experimental case studies," *IEEE J. Quantum Electron.*, vol. 25, pp. 2239–2254, 1989.

[5] A. Takemoto *et al.*, "Low harmonic distortion distributed feedback laser diode and module for CATV systems," in *Tech. Dig. OFC'90*, pp. 214.

[6] G. Morthier, P. Vankwikelberge, F. Buytaert, R. Baets, and P. Lagasse, "Linewidth of single mode DFB lasers in the presence of spatial and spectral hole burning," in *Proc. European Conf. Opt. Commun. ECOC 89* (Gothenburg, Sweden).

[7] G. Agrawal and A. Bobeck, "Modeling of distributed feedback semiconductor lasers with axially varying parameters," *IEEE J. Quantum Electron.*, vol. 24, pp. 2407–2414, 1988.

[8] T. Kimura and A. Sugimura, "Linewidth reduction by coupled phase-shift distributed feedback laser," *Electron. Lett.*, vol. 23, pp. 1014–1015, 1987.

[9] P. Zhou and G. S. Lee, "Mode selection and spatial hole burning suppression of a chirped grating distributed feedback laser," *Appl. Phys. Lett.*, vol. 56, pp. 1400–1402, 1990.

[10] G. Morthier, P. Vankwikelberge, K. David, and R. Baets, "Improved performance of AR-coated DFB-lasers by the introduction of gain coupling," *IEEE Photon. Technol. Lett.*, vol. 2, pp. 170–172, Mar. 1990.

[11] H. Kogelnik and C. V. Shank, "Coupled-wave theory of distributed feedback lasers," *J. Appl. Phys.*, vol. 43, pp. 2327–2335, 1972.

[12] T. Schrans and A. Yariv, "Semiconductor lasers with uniform longitudinal intensity distribution," *Appl. Phys. Lett.*, vol. 56, pp. 1526–1528, 1990.

[13] G. Morthier, K. David, P. Vankwikelberge, and R. Baets, "A new DFB laser diode with reduced spatial hole burning," *IEEE Photon. Technol. Lett.*, vol. 2, pp. 388–390, June 1990.

[14] G. Heise, R. Matz, and U. Wolff, "Phase-shifted holographic gratings for distributed feedback lasers," *SPIE Integrated Optical Circuits*, Vol. 651.

[15] D. C. J. Reid *et al.*, "Moiré fibre grating resonators," *MOC/GRIN '89*, PD5, pp. 19-22, Tokyo.

*

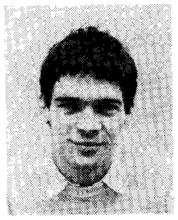

Geert Morthier was born in Gent, Belgium, on March 20, 1964. He received the degree in electrical engineering from the University of Gent, Belgium, in 1987. Since 1988, after serving one year in the army, he has been working toward the Ph.D. degree in electrical engineering at the Laboratory of Electromagnetism and Acoustics, University of Gent. His main research interests are the spectral and dynamic properties of semiconductor lasers, and of DFB lasers in particular.

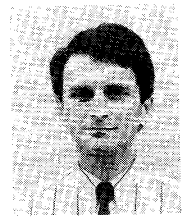

Roel Baets (M'88) received the degree in electrical engineering from the University of Gent, Belgium, in 1980. He received the M.Sc. degree in electrical engineering from Stanford University, Stanford, CA, in 1981 and the Ph.D. degree from the University of Gent in 1984.

From 1984 to 1989 he was employed by the Interuniversity Micro-Electronics Centre (IMEC) and worked in the Laboratory of Electromagnetism and Acoustics at the University of Gent, where he coordinated the optoelectronic device research. Since 1989 he has been a professor at the University of Gent. Since 1990 he has also been a part-time professor at the Technical University of Delft, The Netherlands.

Dr. Baets is a member of the Optical Society of America and the Flemish Engineers Association.